Simple and complex micelles in amphiphilic mixtures: a coarse-grained mean-field study

Martin J. Greenall

*Institut Charles Sadron, 23, rue du Loess, 67034 Strasbourg, France**

Gerhard Gompper

Theoretical Soft Matter and Biophysics, Institute for Complex Systems, Forschungszentrum Jülich, 52425 Jülich, Germany

Abstract

Binary mixtures of amphiphiles in solution can self-assemble into a wide range of structures when the two species individually form aggregates of different curvatures. In this paper, we focus on small, spherically-symmetric aggregates in a solution of sphere-forming amphiphile mixed with a smaller amount of lamella-forming amphiphile. Using a coarse-grained mean-field model (self-consistent field theory, or SCFT), we scan the parameter space of this system and find a range of morphologies as the interaction strength, architecture and mixing ratio of the amphiphiles are varied. When the two species are quite similar in architecture, or when only a small amount of lamella-former is added, we find simple spherical micelles with cores formed from a mixture of the hydrophobic blocks of the two amphiphiles. For more strongly mismatched amphiphiles and higher lamella-former concentrations, we instead find small vesicles and more complex micelles. In these latter structures, the lamella-forming species is encapsulated by the sphere-forming one. For certain interaction strengths and lamella-former architectures, the amount of lamella-forming copolymer encapsulated may be large, and the implications of this for the solubilization of hydrophobic chemicals are considered. The mechanisms behind the formation of the above structures are discussed, with a particular emphasis on the sorting of amphiphiles according to their preferred curvature.

*Electronic address: mjgreenall@physics.org

I. INTRODUCTION

Amphiphilic molecules such as block copolymers and lipids can self-assemble into many different structures when dissolved in solution [1, 2]. This phenomenon has recently attracted a great deal of attention [3, 4], driven both by the potential applications of self-assembled amphiphile aggregates in the encapsulation and delivery of active chemicals such as drugs and genetic material [5, 6] and the insights gained into biological systems [7].

For solutions of a single type of simple amphiphile, such as a diblock copolymer or simple lipid, it is fairly straightforward to gain a basic understanding of which aggregate will form in a given system [8, 9]. Although a variety of factors, such as the concentration [8, 10] and size [11] of the amphiphilic molecules, may play a role, the shape of the aggregates is most easily controlled via the architecture of the amphiphile; that is, the relative sizes of its hydrophilic and hydrophobic blocks. If the hydrophilic component is large (or appears large due to its interaction with the solvent), then spherical micelles are seen. However, if the hydrophobic block is large, lamellar structures such as vesicles form. For intermediate architectures, cylindrical micelles are observed, either as isolated, worm-like structures [12], or branched networks [13].

The experimental phenomenology is much richer in binary mixtures of amphiphiles [14], especially those that individually self-assemble into different aggregates [15–17]. Novel structures are observed, such as undulating cylinders and branched, octopus-like aggregates [15]. Binary mixtures have been investigated in a wide variety of amphiphile systems. A great deal of work has been carried out on lipid-detergent systems [18, 19], and over the past few years lipid [7, 20, 21] and block copolymer [12, 15] mixtures have been widely studied. Lipid mixtures are of interest due to their presence in cells and role in biological transport processes [22]. In the case of block copolymers, on the other hand, the motivation for the use of two amphiphiles is that it greatly increases the number of design parameters and gives finer control over the self-assembly. The architectures and concentrations of both species may now be varied, as may the stage in the self-assembly process at which they are blended [12]. A number of properties of the aggregates may be controlled, such as their shape [12], stability [23], and ability to solubilize hydrophobic compounds [24]. An interesting and recent example is the addition of lamella-forming copolymers with a short hydrophilic block to a solution of longer sphere-formers to increase the solubilization capacity of the resulting

micelles while maintaining their compact and stable spherical shape [23, 24]. In the current paper, we study a basic example of such a system: a solution of sphere-forming diblock copolymers to which an admixture of diblocks with a much shorter hydrophilic block is added. To study the problem in as simple a form as possible, we consider two copolymer species that are formed of the same species A (hydrophilic) and B (hydrophobic), and have the same length hydrophobic blocks. We focus on the case where the sphere-formers remain in the majority, and, using coarse-grained mean-field theory, investigate how the small spherical aggregates formed are modified by the presence of the shorter copolymers. We perform a broad scan of the system's parameter space, and study how the core composition and radius of the micelles are affected by the interactions, concentrations and architectures of the two polymers.

The paper is organized as follows. In the following section, we introduce the coarse-grained mean-field theory (self-consistent field theory) that will be used. We then present and discuss our theoretical results, and give our conclusions in the final section.

II. SELF-CONSISTENT FIELD THEORY

Self-consistent field theory (SCFT) [25] is a coarse-grained mean-field model that has been used successfully to model equilibrium [26–28] and metastable [29, 30] structures in polymers blends and melts. SCFT has several features that make it particularly suitable for the study of the current problem of small binary aggregates. First, its general advantages are that it is less computationally intensive than simulation techniques such as Monte Carlo, yet, for sufficiently long amphiphiles [31], provides comparably accurate predictions of micelle size and shape [31–33]. Secondly, as a relatively simple, coarse-grained theory, it will allow us to model the broad phenomenology of the system clearly and show how general the phenomena observed are likely to be. Furthermore, SCFT has a specific feature that is especially useful in the current problem: it makes no initial assumption about the segregation of two copolymers of different architecture within the micelle, provided the two amphiphile species are formed from the same types of monomer. This will enable us to demonstrate that effects such as the encapsulation of one polymer species by another within the micelle arise spontaneously and do not require further assumptions to be made.

To make our discussion more concrete, we now outline the mathematical structure and

main assumptions of SCFT as applied to the current system. The theory considers an ensemble of many polymers. These are modeled as random walks in space, which means that fine details of their molecular structure are not taken into account [34]. The inter-molecular interactions are modeled by assuming that the system is incompressible and introducing a contact potential between the molecules [28], the strength of which is fixed by the Flory χ parameter [35].

The first step in finding an approximation method (SCFT) for this problem is to think of each polymer molecule as being acted on by a field produced by all other molecules in the system [28]. Viewing the problem in this way involves no approximations in itself, but has several advantages when computing numerical solutions. First, it transforms the N-body problem of modeling a system of N polymers into N 1-body problems [28]. The advantage of this arises from the fact that, since we are interested in computing average properties, we consider the partition sum over all possible system configurations. This means that all molecules of a given species may be treated as equivalent and we in fact only have to solve one 1-body problem for each type of polymer in the system. Second, this approach allows us to replace the discrete sum over the system configurations by a continuous integral over smooth functions, which is easier to deal with numerically [30]. Finally, the computational burden of the problem may be sharply reduced by finding approximate forms of the field variables using a saddle-point (mean-field) approximation [34], which corresponds to neglecting fluctuations in the system.

SCFT can be used to study a wide variety of polymer systems, including simple homopolymers [36], more complex copolymers [37, 38] and mixtures of these [39]. We now outline the application of SCFT to our current system of two amphiphiles in a solvent, which we model by a simple mixture of two types of AB block copolymer with A homopolymer solvent. We take the lamella-forming species of copolymer to have a mean-squared end-to-end distance of a^2N, where a is the monomer length and N is the degree of polymerization [28]. This polymer contains N_B hydrophobic B-monomers and $N_\mathrm{A} = N - N_\mathrm{B}$ hydrophilic A-monomers. To consider the effect of different lamella-formers on the self-assembly, we vary the number of A monomers while keeping N_B fixed.

We note that our use of the term lamella-former to refer to amphiphiles with short hydrophilic blocks is not precise, as these molecules might precipitate rather than self-assemble in solution [40] if not mixed with an amphiphile with a larger hydrophilic block

such as a sphere-former. Furthermore, in aggregates formed from a mixture of sphere-formers and amphiphiles with a short hydrophilic block, the presence of these latter molecules might lead to the formation of regions of negative curvature rather than the zero-curvature regions that would be favored by a lamella-former.

All sphere-formers considered contain $N_{\mathrm{B2}} \equiv N_{\mathrm{B}}$ hydrophobic monomers, but their overall length is necessarily greater and is given by αN, where $\alpha > 1$. As above, the number of A monomers N_{A2} is varied with N_{B} fixed in order to investigate the effect of sphere-former architecture on the aggregate properties. For simplicity, the number N_{S} of A monomers in a homopolymer solvent molecule is also fixed at N_{B}. Since we focus on spherical aggregates, we assume spherical symmetry of the calculation box with reflecting boundary conditions at the origin and outer limit of the system.

In this paper, we keep the amounts of copolymer and homopolymer fixed; that is, we work in the canonical ensemble. Applying the procedure described above, we find that the SCFT approximation to the free energy of our system has the form

$$\begin{aligned}\frac{FN}{k_{\mathrm{B}}T\rho_0 V} &= \frac{F_{\mathrm{h}}N}{k_{\mathrm{B}}T\rho_0 V} \\ &- (\chi N/V)\int \mathrm{d}\mathbf{r}\,\left[(\phi_{\mathrm{A}}(\mathbf{r})+\phi_{\mathrm{A2}}(\mathbf{r})+\phi_{\mathrm{S}}(\mathbf{r})-\overline{\phi}_{\mathrm{A}}-\overline{\phi}_{\mathrm{A2}}-\overline{\phi}_{\mathrm{S}})(\phi_{\mathrm{B}}(\mathbf{r})+\phi_{\mathrm{B2}}(\mathbf{r})-\overline{\phi}_{\mathrm{B}}-\overline{\phi}_{\mathrm{B2}})\right] \\ &- (\overline{\phi}_{\mathrm{A}}+\overline{\phi}_{\mathrm{B}})\ln(Q_{\mathrm{AB}}/V) - [(\overline{\phi}_{\mathrm{A2}}+\overline{\phi}_{\mathrm{B2}})/\alpha]\ln(Q_{\mathrm{AB2}}/V) - \overline{\phi}_{\mathrm{S}}\ln(Q_{\mathrm{S}}/V) \qquad (1)\end{aligned}$$

where the $\overline{\phi}_i$ are the mean volume fractions of the various components. The $\phi_i(\mathbf{r})$ are the local volume fractions, with $i = A$ or $A2$ for the hydrophilic components of species 1 and 2, $i = B$ or $B2$ for the hydrophobic components and $i = S$ for the A homopolymer solvent. The strength of the repulsive interaction between the A monomers (hydrophilic component and solvent) and B monomers (hydrophobic component) is determined by the Flory parameter χ. V is the total volume, $1/\rho_0$ is the volume of a monomer, and F_{h} is the SCFT free energy of a homogeneous system of the same composition. This last quantity contains terms arising from the entropy of mixing of the different species [35] and a term proportional to χ describing the interactions of the species in the absence of self-assembly [28]. The architectures of the individual molecules enter through the single-chain partition functions Q_i. As an example, that for the homopolymer is given by [28]

$$Q_{\mathrm{S}}[w_{\mathrm{A}}] = \int \mathrm{d}\mathbf{r}\, q_{\mathrm{S}}(\mathbf{r},s)q_{\mathrm{S}}^{\dagger}(\mathbf{r},s) \qquad (2)$$

where the q and $q^\dagger$ terms are single chain propagators [28]. The partition functions of the copolymer chains are calculated in a similar way. We now recall that the polymer molecules are modeled as random walks in an external field that describes their interactions with the other molecules in the system. This is reflected in the fact that the propagators satisfy diffusion equations with a field term. Again considering the case of the homopolymer, we have

$$\frac{\partial}{\partial s} q_{\mathrm{S}}(\mathbf{r}, s) = \left[\frac{1}{6} a^2 N \nabla^2 - w_{\mathrm{A}}(\mathbf{r}) \right] q_{\mathrm{S}}(\mathbf{r}, s) \tag{3}$$

where s is a curve parameter specifying the position along the polymer and the initial condition is $q_{\mathrm{S}}(\mathbf{r}, 0) = 1$. The copolymer propagators are computed similarly, although in this case the corresponding diffusion equation is solved with the field $w_i(\mathbf{r})$ and the prefactor of the $\nabla^2 q$ term appropriate to each of the two sections of the copolymer [41]. In the case of the longer sphere-forming copolymer, the fields must be multiplied by the ratio α to take into account the higher degree of polymerization [28].

The derivation of the mean-field free energy F also generates a set of simultaneous equations linking the values of the fields and densities. The first of these simply states that all volume fractions must add to 1 at all points due to the incompressibility of the system; however, we also find the following linear relation

$$w_{\mathrm{A}}(\mathbf{r}) - w_{\mathrm{B}}(\mathbf{r}) = 2\chi N[\overline{\phi}_{\mathrm{A}} + \overline{\phi}_{\mathrm{A2}} + \overline{\phi}_{\mathrm{S}} - \phi_{\mathrm{A}}(\mathbf{r}) - \phi_{\mathrm{A2}}(\mathbf{r}) - \phi_{\mathrm{S}}(\mathbf{r})] \tag{4}$$

Furthermore, the homopolymer density is related to the propagators (see Eqn. 3) according to [28]

$$\phi_{\mathrm{S}}(\mathbf{r}) = \frac{V \overline{\phi}_{\mathrm{S}}}{Q_{\mathrm{S}}[w_{\mathrm{A}}]} \int_0^1 \mathrm{d}s \, q_{\mathrm{S}}(\mathbf{r}, s) q_{\mathrm{S}}^\dagger(\mathbf{r}, s) \tag{5}$$

The copolymer densities are computed in a similar way, with the integration limits set to give the required amounts of each species.

In order to calculate the SCFT density profiles for a given set of polymer concentrations, Eqn. 4 must be solved with the densities calculated as in Eqn. 5 and taking account of the incompressibility of the system. To begin, we make a initial guess for the fields $w_i(\mathbf{r})$ with the approximate form of a micelle and solve the diffusion equations to calculate the propagators and then the densities corresponding to these fields (see Eqns 3 and 5). New values for the fields are now calculated using the new $\phi_i(\mathbf{r})$, and the w_i are updated accordingly [42]. The procedure is repeated until convergence is achieved.

The diffusion equations are solved using a finite difference method [43]. To resolve the more complex features of the micelle density profiles, it is necessary to use a relatively fine discretization: a spatial step size of $0.028\,aN^{1/2}$ and a step size for the curve parameter s of 0.0025.

Until now, we have only considered isolated spherical micelles. We must now link the thermodynamics of a single aggregate to those of a larger system containing many micelles. To do this, we proceed as follows [44, 45]. Firstly, we calculate the free-energy density of a box containing a single spherical aggregate surrounded by solvent. Since we assume spherical symmetry, the calculation is effectively one-dimensional. The volume of the simulation box containing the aggregate is then varied, keeping the volume fraction of copolymer constant, until the box size with the minimum free-energy density is found. Provided the system is dilute, so that micelle is surrounded by a large volume of solvent, this mimics the behavior of a larger system (of fixed volume and fixed copolymer volume fraction) containing many micelles. The reason for this is that such a system minimizes its total free energy by changing the number of micelles and therefore the volume ('box size') occupied by each. Minimizing the free energy density in this way locates the micelle that would have the lowest free energy and hence be most likely to be observed in a sample containing many aggregates. This approach allows many-micelle systems to be investigated using inexpensive one-dimensional calculations on single aggregates, and its predictions on micelle radii and shape transitions often agree well with experiment [44, 45].

III. RESULTS AND DISCUSSION

We divide the results section into four subsections. These focus on the effect on the micelle morphology of, respectively, the lamella-former concentration, the strength of the interaction between the two species, the lamella-former architecture and the sphere-former architecture.

A. Effect of lamella-former concentration

To begin, we investigate the effect of the gradual addition of lamella-former to a system of sphere-formers, finding the micelle of lowest free energy using the method of variable

subsystem size described above. To see the effect of blending two species as clearly as possible, we consider a pair of strongly mismatched copolymers: a lamella-former with $N_{\mathrm{A}} = N_{\mathrm{B}}/4$ and a sphere-former with $N_{\mathrm{A2}} = 7N_{\mathrm{B}}$. The Flory parameter is set to $\chi N_{\mathrm{B}} = 22.5$, a high value which causes relatively sharp interfaces to form between the species A and B. We fix the overall volume fraction of copolymer to 10%, to give a reasonable volume of solvent around the micelle without making the simulation box so large that the calculations become slow.

Figure 1 shows a series of radial cuts through the density profile of the optimum spherical aggregate as the volume fraction of lamella-former is increased from 5% to 35% of all copolymers in steps of 10%. For the lowest of these lamella-former concentrations (Figure 1a), the sphere-formers and lamella-formers are homogeneously mixed in the core, and a simple mixed micelle is formed (see the sketch in Figure 2). This structure is little different from that which would be formed in a system of pure sphere-forming amphiphiles: the concentration of lamella-formers is not yet sufficiently large to have a strong effect on the micelle morphology. Indeed, for such low lamella-former concentrations, mixed micelles may not be present [46], with pure aggregates of the two species forming instead.

However, as more lamella-forming molecules are added (Figure 1b), their influence on the core composition of the micelle becomes clear. A polymer with a large hydrophobic component that naturally forms flat bilayers or even structures of negative curvature is in an energetically highly unfavorable state in a small, positively curved micelle. In consequence, these molecules segregate to the center of the aggregate, where they form a tightly-wrapped bilayer. This structure is sketched in Figure 3. The polymers in the inner leaflet of this bilayer are in a more favorable negative curvature state, with their hydrophilic components pointing in towards the center of the micelle. Those in the outer leaflet are also in a more favorable state than at lower lamella-former concentrations: they are no longer forced into the core of a compact micelle, but sit in a shell on the outside of the new core region. Here, they are mixed with the sphere-formers, which can no longer form their preferred simple micelle structure, but strongly prefer the positively-curved surface of the new spherical aggregate to its core. The new micelle therefore has an inner core of hydrophilic A-blocks, an outer core of hydrophobic B-blocks, and a hydrophilic A corona.

As the lamella-former concentration is increased still further, to 25% by volume of all copolymers (Figure 1c), solvent penetrates into the core of the micelle, as the inner bilayer

of lamella-formers becomes more dominant in fixing the micelle morphology and expands towards the planar state. This process continues in Figure 1d, where 35% of all copolymers are lamella-forming. Here, a number of the sphere-formers have mixed with the inner leaflet of the lamella-former bilayer, meaning that the overall structure has the form of a (very) small bilayer vesicle (see the sketch in Figure 4). Small vesicles with a preferred radius have indeed been seen in experiments on mixtures of sphere- and lamella-forming amphiphiles [7, 47]. Their existence has also been predicted in recent lattice SCFT calculations by Li et al. [48]. Our current work considers a different region of parameter space to these lattice-based calculations, which focus on weakly mismatched amphiphiles and (usually) higher lamella-former concentrations. In consequence, the mechanism by which the preferred vesicle radius is selected appears to be rather different in the two studies. In our work, strong segregation of the two species occurs and the compositions of the inner and outler leaflets of the bilayer are quite different. The small vesicle structure forms as it accommodates both the preference of the shorter copolymers for a bilayer structure and that of the longer, sphere-forming amphiphiles for positively-curved surfaces. This is in contrast to the results of Li et al. [48], where the vesicles are larger and the two bilayer leaflets have similar compositions. The individual vesicles therefore have no preferred curvature, and coexistence with a high concentration of mixed micelles is found to be necessary for vesicle size selection to occur. Highly-curved mixed bilayers may also be seen as the end sections of larger tubular vesicles [49], and have also been investigated using molecular dynamics simulations [50]. Our current work gives some broad guidance as to how the system parameters might be varied in order to encourage or discourage the formation of these structures.

We now turn our attention to a system in which the two polymer species have the same architectures as before ($N_{\mathrm{A}} = N_{\mathrm{B}}/4$ for the lamella-former and $N_{\mathrm{A2}} = 7N_{\mathrm{B}}$ for the sphere-former), but a significantly weaker interaction strength of $\chi N_{\mathrm{B}} = 15$. The difference between the two systems can be seen even at only 5% lamella-former (Figure 5a). Here, the radial segregation of the two polymers according to their preferred curvatures is already clearly underway. Before, it was prevented at lower lamella-former concentrations by the energetic cost of mixing the hydrophilic A blocks with the hydrophobic B core. As more lamella-former is added to reach 15% (Figure 5b), the behavior of the two systems diverges still further. In the system with stronger repulsive interactions discussed earlier, the A and B blocks demix in the core, leading to the ABA structure seen in Figure 1b and sketched in

Figure 3. In the current system, although some demixing does indeed occur (Figure 5b), the effect is much weaker, and A- and B-rich regions can no longer be clearly separated. This structure is sketched in Figure 6. For even larger concentrations of lamella-former of 25% and 35% (Figure 5c and d), the small vesicle structure seen before is absent. Instead, since the A and B blocks may mix much more freely than before, the core of the micelle is formed of a nearly homogeneous melt of lamella-former.

To make our study of the concentration dependence of the binary system more quantitative, we calculate the core radius and composition as a function of the ratio ϕ'/ϕ of the volume fraction of lamella-formers ϕ' to the total volume fraction of copolymers ϕ. We define the core boundary as the radius at which the volume fraction of hydrophobic blocks is equal to 0.5, and plot this quantity in Figure 7a for both systems considered above. The core radii of both species grow steadily and almost identically as the lamella-former concentration is increased. In the case of the system with $\chi N_{\mathrm{B}} = 22.5$, the growth is associated with the expansion of the micelle to form a small vesicle, while in the system with weaker interactions ($\chi N_{\mathrm{B}} = 15$), it arises from the fact that the core is gradually filling with lamella-former. The only appreciable difference in radius is seen in the final point, where 40% of all copolymers are lamella-forming. Here, the radius of the $\chi N_{\mathrm{B}} = 22.5$ system has begun to grow more rapidly, as the system moves towards the planar bilayer state. For lamella-former fractions greater than 40%, the influence of the sphere-forming copolymers is weak, and we were no longer able to find free-energy minima corresponding to small spherical aggregates.

The contrast between the high and low interaction strength systems emerges more clearly if we consider the amounts of the different species in the core defined above. The upper two curves in Figure 7b show the fraction of the core that is composed of A-blocks for each of the two systems, while the lower two curves show the fraction of the core that is composed of homopolymer solvent. In the $\chi N_{\mathrm{B}} = 15$ system, the amount of A-block in the core grows steadily as the amount of lamella-former is increased, as in this case the lamella-forming copolymer is simply encapsulated in the center of the micelle. For low lamella-former concentrations, the $\chi N_{\mathrm{B}} = 22.5$ system forms simple micelles with a clear interface in between the core and corona, and so has less A-block in the core than does the $\chi N_{\mathrm{B}} = 15$ system, where some mixing of A and B blocks occurs in the core. In contrast, for larger amounts of lamella-forming copolymer, the fraction of A-block in the more strongly-interacting system grows more and more rapidly as the preferred aggregate changes from a

closed micelle to an open vesicle.

The clearest difference between the two systems is seen in the behavior of the amount of solvent in the core as the lamella-former concentration is increased (see the lower two curves in Figure 7b). In the $\chi N_{\mathrm{B}} = 15$ system, where the core is largely composed of copolymers, the fraction of solvent remains fairly constant at around 0.02-0.03. The fact that this value is a little higher than might be expected from the density profiles in Figure 5, and also varies slightly, can be attributed to the fact that our simple definition of the core radius means that a thin shell of solvent is always included as part of the core. In the system with stronger repulsion between the A and B components, the core solvent fraction starts at a similar small value, remaining close to this as the lamella-former volume fraction is increased and the morphology of the system changes from a simple micelle to the ABA structure shown in Figure 3. However, as the fraction of lamella-formers ϕ'/ϕ is increased towards 40%, the fraction of solvent in the core grows very quickly as the aggregate expands towards a vesicle.

We have checked a selection of these calculations for a much more dilute system with an overall copolymer volume fraction of $\phi \approx 1\%$, focusing in particular on those lamella-former volume fractions where the aggregate changes from one morphology to another. Such a dilute system may be more appropriate for observation of the small spherical structures considered in this paper, since a more concentrated solution might form larger aggregates such as worm-like micelles. We therefore wish to check that the form of the optimum spherical aggregates is not strongly sensitive to concentration (although the likelihood of their formation with respect to larger aggregates may of course depend on the concentration).

Indeed, little change in the form of the aggregates is observed. The most significant difference is that, in the dilute case, the transition between the simple micelle and the ABA structure in the $\chi N_{\mathrm{B}} = 22.5$ system occurs when ϕ'/ϕ is between 15% and 20%, rather than between 10% and 15% in the $\phi = 10\%$ system. This preference for small spherical micelles in more dilute systems is in line with the known concentration dependence of block copolymer solutions [8]. Similar small shifts in the morphology transitions as the overall copolymer concentration is varied, or no appreciable shifts at all, are observed in all the systems considered in this paper, where the polymers considered aggregate reasonably strongly and the free-energy minima associated with the various micelle shapes will be relatively sharp. This is not the case for shorter or more weakly-interacting polymers, where the concentration dependence may be quite strong.

B. Effect of interaction strength

In the results discussed in the preceding subsection, we found a clear contrast in phenomenology between two systems with different levels of repulsion between their hydrophilic and hydrophobic components. To investigate this effect in more detail, we take a system with the same copolymer architectures as considered above ($N_{\mathrm{A}} = N_{\mathrm{B}}/4$ for the lamella-former and $N_{\mathrm{A2}} = 7N_{\mathrm{B}}$ for the sphere-former), fix the lamella-former fraction ϕ'/ϕ to 25%, and vary χN_{B}. Figure 8 shows a series of cuts through the density profiles of the small spherical aggregates formed as χN_{B} is increased from 15 to 30 in steps of 5. For the smallest of these values, shown in Figure 8a, we find a weakly-structured aggregate of the kind shown in Figure 5. Very similar results are also found for the even smaller value of $\chi N_{\mathrm{B}} = 12.5$. Below this value, no self-assembly takes place.

As χN_{B} is increased to 20 (Figure 8b), the segregation between hydrophilic and hydrophobic blocks has become much stronger, and the ABA aggregate of Figure 3 is seen, with some penetration of solvent into the core region. On further increase of χN_{B}, the boundaries between the various layers become sharper and sharper as the repulsive interaction between the A and B blocks increases in strength. The radius also increases, and the aggregate opens out to a small vesicle. Finally, in Figure 8d, where $\chi N_{\mathrm{B}} = 30$, the layers are very clearly defined, and the calculated density profile resembles very closely the vesicle sketched in Figure 4.

C. Effect of lamella-forming architecture

In the two previous subsections, we considered the effect of blending two strongly mismatched copolymers, to demonstrate the effects of segregation on the micelle morphologies as clearly as possible. We now investigate how the micelle shapes change as the mismatch between the two polymers is decreased. Specifically, the hydrophilic block size of the lamella-former is gradually increased from the small value $N_{\mathrm{A}} = N_{\mathrm{B}}/4$ used in the preceding calculations until we reach the symmetric molecule with $N_{\mathrm{A}} = N_{\mathrm{B}}$. The same sphere-former architecture as before is used, with $N_{\mathrm{A2}} = 7N_{\mathrm{B}}$. Since we wish to focus specifically on the effects of the lamella-former, we use a slightly higher fraction of these molecules than in the preceding section, and set $\phi'/\phi = 33.3\%$.

To begin, we set $\chi N_B = 15$, and first consider the strong lamella-former with $N_A = N_B/4$. This is the system of Figure 5, and, as there, we find large micelles with a weakly-structured core (see Figure 9 a). A sharp change is observed when the length of the hydrophilic component of the lamella-forming copolymer is increased to $N_A = 3N_B/7$ (Figure 9b). Here, the AB interfaces within the core become well-defined, and the ABA aggregate sketched in Figure 3 is seen, with some penetration of solvent into the core. This indicates that the formation of the weakly-structured aggregate seen in Figure 9a requires not only a relatively small χ parameter between the hydrophilic and hydrophobic blocks, but also a short hydrophilic block of the lamella former. If the length of this block is increased, the effective strength χN of the interaction between the A and B blocks of the lamella-former becomes larger [35] and the two blocks can segregate within the core.

As the length of the hydrophilic block of the lamella-former is increased still further, to $N_A = 2N_B/3$, the mismatch between the two species decreases and the aggregate shows the first signs of approaching the small micelle favored by the sphere-formers. Specifically, the core radius decreases slightly, and the solvent begins to be expelled from the center of the micelle (Figure 9c). This process is complete in Figure 9d, where the lamella former is symmetric and $N_A = N_B$. Here, a simple mixed micelle is formed, with no segregation of the two species.

We now consider a system with the same sequence of polymer architectures as above, but with a larger repulsive interaction strength $\chi N_B = 22.5$ between the A and B blocks. For the shortest lamella-former, with $N_A = N_B/4$, a small vesicle forms (Figure 10a), in contrast to the weakly-structured aggregate seen for this architecture for the smaller value of χN_B (Figure 9 a). As the hydrophilic block length of the lamella-former is increased, and the degree of mismatch between the two copolymer species lessens, the vesicle contracts (Figure 10b and c) until a simple mixed micelle is formed (Figure 10d).

As in our discussion of the dependence of the micelle morphology on lamella-former concentration, we now plot the aggregate core radii and composition as a function of lamella-former architecture for the two systems studied in this section. In Figure 11a, we show the decrease of the micelle radius as the length of the lamella-former hydrophilic block is increased. The lower line shows the behavior of the radius of the system with the smaller Flory parameter $\chi N_B = 15$. The sharpest change in the radius occurs between the first two points, when the aggregate changes from the weakly segregated structure plotted in

Figure 9a to an ABA micelle with the form shown in Figure 9b. This latter structure then gradually contracts as the lamella-former is lengthened until we arrive at the simple mixed micelle plotted in Figure 9d. This steady contraction with increasing lamella-former length is also seen in the $\chi N_B = 22.5$ system. The small vesicle/ABA morphology is especially robust here, being formed not only for the short lamella-former (which formed a weakly-structured aggregate for $\chi N_B = 15$) but also for all other lamella-formers apart from the longest with $N_A = N_B$.

The fraction of the core that is composed of A-blocks displays especially interesting behavior as the lamella-former hydrophilic block length is varied. In the system with the smaller Flory parameter $\chi N_B = 15$, the A-block fraction has a rather high value of around 0.125 for the short lamella-formers with $N_A = N_B/4$. This is because the system forms a weakly-structured aggregate (Figure 9a) here, with a core composed of lamella-forming copolymers (Figure 6). As the hydrophilic blocks of the lamella-formers are lengthened, solvent enters into the core and the A-block fraction falls slightly. Further increase of the lamella-former hydrophilic block length causes the fraction of A-blocks in the core to rise steadily. The reason for this is that, as the aggregate shrinks and solvent is slowly expelled from the center of the aggregate, the amount of A-blocks changes relatively little. These blocks therefore come to constitute a larger fraction of the core. As the lamella-former A-blocks are lengthened still further, we observe a sharp drop in the fraction of hydrophilic material in the core, as the system contracts to form a simple mixed micelle.

Some aspects of this behavior are also seen in the $\chi N_B = 22.5$ solution. Here, the weakly-structured aggregate of Figure 9a is not present, and the system forms a small vesicle in the case of the shortest lamella-formers. As the A-block length of these molecules is increased, the amount of solvent in the core of the aggregate decreases, and the fraction of A-blocks in the core rises, as in the case of the $\chi N_B = 15$ system. For the largest A-block lengths studied, the fraction of hydrophilic material in the core is much smaller, as the system has formed a mixed micelle with a predominantly hydrophobic core.

To reinforce the above arguments, we also show in Figure 11b the volume fraction of the core that is composed of solvent as a function of lamella-former hydrophilic block length. For the solution with $\chi N_B = 15$, the core solvent fraction initially rises as the weakly segregated structure is replaced by an ABA structure with some solvent in the core. It then falls gradually as the aggregate contracts to form a mixed micelle. A similar steady fall

is observed in the more strongly segregated $\chi N_{\rm B} = 22.5$ system, as the small open vesicle observed for small $N_{\rm A}$ closes to form a micelle.

D. Effect of sphere-forming architecture

To conclude the scan of our system's parameter space, we now investigate the effect of the architecture of the sphere-former on the morphology of the aggregates. In the above results, we focused on strongly mismatched copolymers and so used a highly asymmetric sphere-former with $N_{\rm A2} = 7N_{\rm B}$. We now vary the length of the hydrophilic block of the sphere-forming copolymer over a wide range, starting from a short molecule with $N_{\rm A2} = 3N_{\rm B}$ and increasing the number of A monomers until $N_{\rm A2} = 9N_{\rm B}$. The architecture of the lamella-former is fixed, with $N_{\rm A} = N_{\rm B}/4$, and, as in all the above cases, the total copolymer volume fraction is kept constant at 10%. Three quarters of these copolymers are sphere-forming, so that $\phi'/\phi = 25\%$. As in our studies of the effect of copolymer concentration and lamella-former architecture, we consider two values of the Flory parameter: $\chi N_{\rm B} = 22.5$ and $\chi N_{\rm B} = 15$.

In Figure 12a to d, we show cuts through the density profiles of the optimum aggregates formed when $N_{\rm A2} = 3N_{\rm B}$, $5N_{\rm B}$, $7N_{\rm B}$ and $9N_{\rm B}$ for $\chi N_{\rm B} = 15$. Despite the wide variation in the number of hydrophilic monomers, roughly similar small vesicle structures are formed in all cases, with particularly little change in morphology being observed between $N_{\rm A2} = 5N_{\rm B}$ and $9N_{\rm B}$. Provided the two copolymer species are sufficiently strongly mismatched to segregate within the aggregate, there is indeed no reason to suspect that increasing the sphere-former A-block length further should cause major qualitative changes to the form of the aggregate, as the sphere-formers have already reached the outer surface and can move no further. In fact, the differences between the four panels of Figure 12 can be attributed mainly to the fact that increasing the length of the sphere-former hydrophilic block at constant ϕ'/ϕ gradually reduces the amount of sphere-former hydrophobic block, with the result that the hydrophobic core becomes more and more dominated by the lamella-former. In consequence, the core radius of the aggregate increases somewhat, as the lamella-formers push outwards towards their preferred flat state.

The dependence of the aggregate shape on the hydrophilic block length of the sphere-formers is similarly weak for the smaller Flory parameter $\chi N_{\rm B} = 15$. Here, aggregates with

the same basic form of an outer layer of sphere-forming copolymers encapsulating a weakly-structured core of lamella-formers are seen for $N_A = 3N_B$, $5N_B$, $7N_B$ and $9N_B$ (Figure 13a-d). As in the $\chi N_B = 22.5$ case, rather little difference in morphology can be seen as the sphere-former hydrophilic block length is increased from $5N_B$ to $9N_B$, save for a fall in the density of the outer sphere-former layer of the core and a slow growth in the core radius. The explanation for these changes is also the same as in the system with a higher Flory parameter. Specifically, the gradual fall in the amount of sphere-former hydrophobic block means that the core becomes predominantly composed of lamella-forming copolymers, which also causes it to swell.

The relative insensitivity to sphere-former architecture observed in both the systems discussed in this section can clearly be seen from plots of the core radius and composition as a function of the sphere-former A-block length (Figure 14). The growth of the core radius shown in Figure 14a is clearly weaker than that seen in the corresponding plots of Figure 7 and Figure 11. Furthermore, the fraction of the core composed of A-blocks (upper lines) or solvent (lower lines) remains rather close to constant, although a weak growth in the amount of solvent in the open structure of Figure 12 can be seen. This is in line with the relatively unchanging morphologies plotted in Figure 12 and Figure 13.

IV. CONCLUSIONS

Using a coarse-grained mean-field approach (self-consistent field theory) we have modeled several aspects of the formation of small, spherically-symmetric aggregates in a solution of sphere-forming amphiphile mixed with a smaller amount of lamella-forming amphiphile. By varying the interaction strength, architecture and mixing ratio of the amphiphiles, we have found a range of morphologies. When the two species were similar in architecture, or when only a small admixture of lamella-forming amphiphile was added, we found simple spherical micelles with purely hydrophobic cores formed from a mixture of the B-blocks of the two amphiphiles. For more strongly mismatched amphiphiles and higher concentrations of lamella-former, we found complex micelles and small vesicles. Specifically, as the concentration of lamella-former was gradually increased in a strongly mismatched system with a relatively high χ parameter, the simple micelle formed at low lamella-former concentrations gradually expanded, first forming a more complex micelle with both A- and B-blocks in

the core and then a small vesicle. For similar systems with lower Flory parameters, the addition of lamella-former resulted in the formation of a intriguing micellar structure in which a large and relatively unstructured core of lamella-former is surrounded by a layer of sphere-forming copolymers. Were this structure able to be stabilized in experiments, it could prove to be useful for the solubilization and delivery of hydrophobic compounds, since it contains a large amount of hydrophobic blocks while retaining a relatively small size. The formation of these aggregates was shown to require not only a relatively weak interaction between the two copolymers, but also for one of the species to have a very short hydrophilic block. The other complex micelles and small vesicles were present over a much wider range of lamella-formers. The architecture of the sphere-formers was found to have a rather weak effect on the aggregate morphology.

The work presented here provides several examples of the wide range of aggregates that may be formed when two amphiphile species that individually self-assemble into aggregates of different curvatures are mixed, and gives broad guidance as to how the polymer parameters might be varied in order to form a given structure. Furthermore, several of the structures shown here show the segregation of amphiphiles according to curvature [7, 20]. Specifically, in many cases, the sphere-forming amphiphiles move to the positively-curved surface of the aggregate. Effectively one-dimensional aggregates such as those considered here are among the simplest possible systems in which this phenomenon could take place.

Several possible extensions of the current work suggest themselves. First, given the potential for the solubilization of hydrophobic chemicals of the large micelles with lamella-former cores, more realistic interaction parameters and modeling of the polymers (if necessary by more microscopic simulation methods) could be carried out in order to search for an experimental parameter range in which these structures could be formed. Such a study could also investigate further the formation of small monodisperse vesicles [7] and bilayers of preferred curvature [49] in binary systems. Second, the study could be extended to mismatched hydrophobic blocks, to allow comparison with recent experiments [51]. Finally, an analogous investigation could be performed for the binary triblock copolymer blends [23, 24] of current interest in drug delivery applications, where large micelles in mixed systems are indeed seen

[23].

[1] S. Jain and F. S. Bates, Science **300**, 460 (2003).

[2] G. Battaglia and A. J. Ryan, J. Phys. Chem. B **110**, 10272 (2006).

[3] T. P. Smart, A. J. Ryan, J. R. Howse, and G. Battaglia, Langmuir **26**, 7425 (2010).

[4] J. R. Howse, R. A. L. Jones, G. Battaglia, R. E. Ducker, G. J. Leggett, and A. J. Ryan, Nat. Mater. **8**, 507 (2009).

[5] Y. Kim, P. Dalhaimer, D. A. Christian, and D. E. Discher, Nanotechnology **16**, S484 (2005).

[6] H. Lomas, I. Canton, S. MacNeil, J. Du, S. P. Armes, A. J. Ryan, A. L. Lewis, and G. Battaglia, Adv. Mater. **19**, 4238 (2007).

[7] A. Zidovska, K. K. Ewert, J. Quispe, B. Carragher, C. S. Potter, and C. R. Safinya, Langmuir **25**, 2979 (2009).

[8] D. J. Kinning, K. I. Winey, and E. L. Thomas, Macromolecules **21**, 3502 (1988).

[9] J. N. Israelachvili, D. J. Mitchell, and B. W. Ninham, J. Chem. Soc. Faraday Trans. 1 **72**, 1525 (1976).

[10] D. J. Adams, C. Kitchen, S. Adams, S. Furzeland, D. Atkins, P. Schuetz, C. M. Fernyhough, N. Tzokova, A. J. Ryan, and M. F. Butler, Soft Matter **5**, 3086 (2009).

[11] H. Kaya, L. Willner, J. Allgaier, and D. Richter, App. Phys. A: Mater. Sci. Process. **74**, S499 (2002).

[12] P. Schuetz, M. J. Greenall, J. Bent, S. Furzeland, D. Atkins, M. F. Butler, T. C. B. McLeish, and D. M. A. Buzza, Soft Matter **7**, 749 (2011).

[13] N. Dan and S. A. Safran, Adv. Colloid Interface Sci. **123**, 323 (2006).

[14] E. W. Kaler, A. K. Murthy, B. E. Rodriguez, and J. A. N. Zasadzinski, Science **245**, 1371 (1989).

[15] S. Jain and F. S. Bates, Macromolecules **37**, 1511 (2004).

[16] S. A. Safran, P. Pincus, and D. Andelman, Science **248**, 354 (1990).

[17] S. A. Safran, P. A. Pincus, D. Andelman, and F. C. MacKintosh, Phys. Rev. A **43**, 1071 (1991).

[18] P. K. Vinson, Y. Talmon, and A. Walter, Biophys. J. **56**, 669 (1989).

[19] J. Oberdisse, O. Regev, and G. Porte, J. Phys. Chem. B **102**, 1102 (1998).

[20] B. Sorre, A. Callan-Jones, J. B. Manneville, P. Nassoy, J. F. Joanny, J. Prost, B. Goud, and P. Bassereau, Proc. Natl. Acad. Sci. U.S.A **106**, 5622 (2009).

[21] M. J. Greenall and G. Gompper, Langmuir **27**, 3416 (2011).

[22] K. Akiyoshi, A. Itaya, S. M. Nomura, N. Ono, and K. Yoshikawa, FEBS Lett. **534**, 33 (2003).

[23] E. S. Lee, Y. T. Oh, Y. S. Youn, M. Nam, B. Park, J. Yun, J. H. Kim, H.-T. Song, and K. T. Oh, Colloids Surf. B **82**, 190 (2011).

[24] K. T. Oh, T. K. Bronich, and A. V. Kabanov, J. Controlled Release **94**, 411 (2004).

[25] S. F. Edwards, Proc. Phys. Soc. **85**, 613 (1965).

[26] P. Maniadis, T. Lookman, E. M. Kober, and K. O. Rasmussen, Phys. Rev. Lett. **99**, 048302 (2007).

[27] F. Drolet and G. H. Fredrickson, Phys. Rev. Lett. **83**, 4317 (1999).

[28] M. W. Matsen, *Soft Matter* (Wiley-VCH, Weinheim, 2006), chap. 2.

[29] D. Duque, J. Chem. Phys. **119**, 5701 (2003).

[30] K. Katsov, M. Müller, and M. Schick, Biophys. J. **87**, 3277 (2004).

[31] A. Cavallo, M. Müller, and K. Binder, Macromolecules **39**, 9539 (2006).

[32] C. M. Wijmans and P. Linse, Langmuir **11**, 3748 (1995).

[33] F. A. M. Leermakers and J. M. H. M. Scheutjens, J. Colloid Interface Sci. **136**, 231 (1990).

[34] F. Schmid, J. Phys.: Condens. Matter **10**, 8105 (1998).

[35] R. A. L. Jones, *Soft Condensed Matter* (Oxford University Press, Oxford, 2002).

[36] A. Werner, M. Müller, F. Schmid, and K. Binder, J. Chem. Phys. **110**, 1221 (1999).

[37] M. Müller and G. Gompper, Phys. Rev. E **66**, 041805 (2002).

[38] J. F. Wang, K. K. Guo, L. J. An, M. Müller, and Z. G. Wang, Macromolecules **43**, 2037 (2010).

[39] N. A. Denesyuk and G. Gompper, Macromolecules **39**, 5497 (2006).

[40] A. M. Mayes and M. O. Delacruz, Macromolecules **21**, 2543 (1988).

[41] G. H. Fredrickson, *The Equilibrium Theory of Inhomogeneous Polymers* (Oxford University Press, Oxford, 2006).

[42] M. W. Matsen, J. Chem. Phys. **121**, 1938 (2004).

[43] W. H. Press, B. P. Flannery, S. A. Teukolsky, and W. T. Vetterling, *Numerical Recipes in C* (Cambridge University Press, Cambridge, 1992), 2nd ed.

[44] M. J. Greenall, D. M. A. Buzza, and T. C. B. McLeish, Macromolecules **42**, 5873 (2009).

[45] M. J. Greenall, D. M. A. Buzza, and T. C. B. McLeish, J. Chem. Phys. **131**, 034904 (2009).

[46] D. F. K. Shim, C. Marques, and M. E. Cates, Macromolecules **24**, 5309 (1991).

[47] F. Li, A. T. M. Marcelis, E. J. R. Sudholter, M. A. C. Stuart, and F. A. M. Leermakers, Soft Matter **5**, 4173 (2009).

[48] F. Li, S. Prevost, R. Schweins, A. T. M. Marcelis, F. A. M. Leermakers, M. A. C. Stuart, and E. J. R. Sudholter, Soft Matter **5**, 4169 (2009).

[49] C. R. Safinya, Colloids Surf. A **128**, 183 (1997).

[50] I. R. Cooke and M. Deserno, Biophys. J. **91**, 487 (2006).

[51] J. Pleštil, C. Koňák, X. Ju, and J. Lal, Macromol. Chem. Phys. **207**, 231 (2006).

Figures

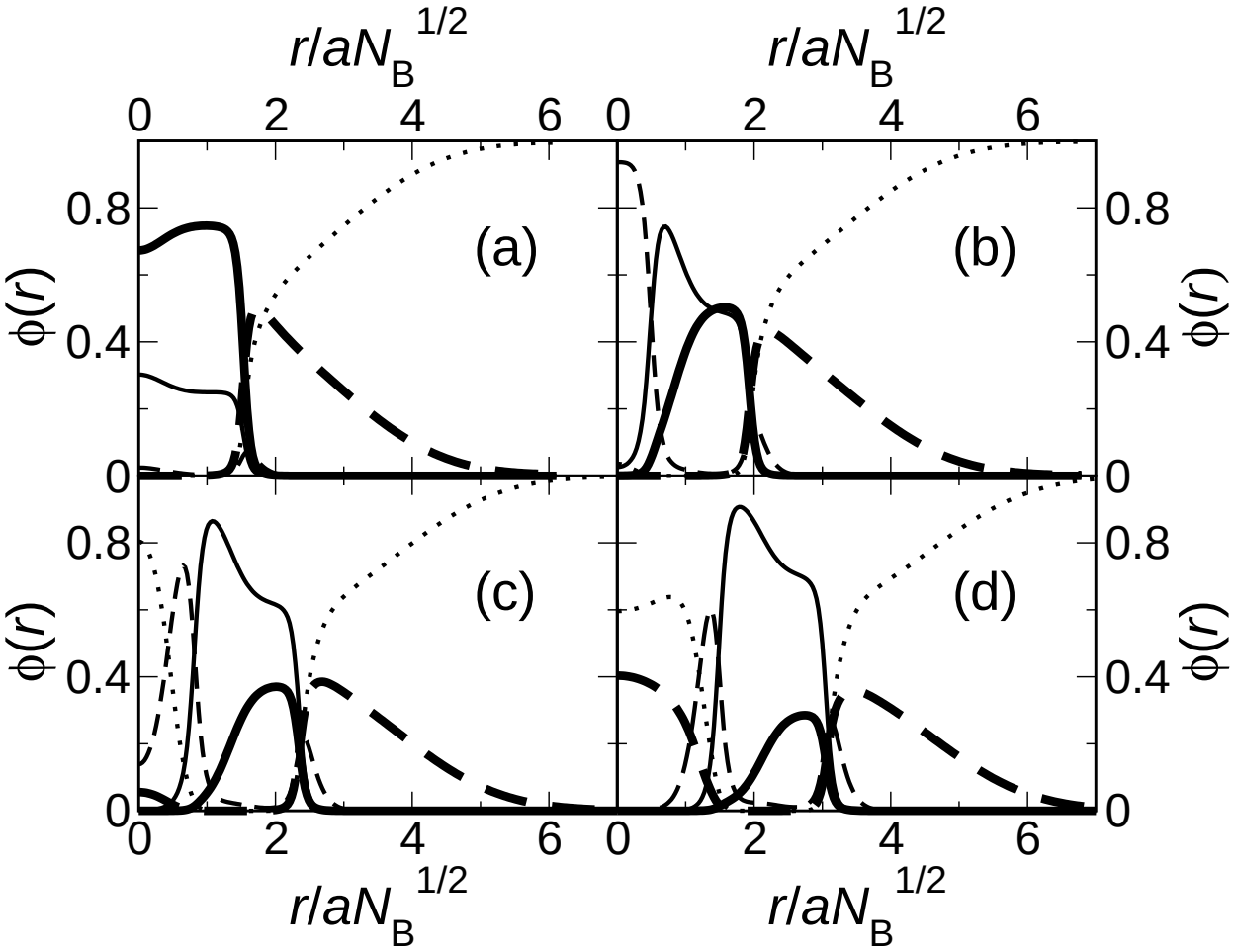

FIG. 1: Cuts through the density profiles of the spherically-symmetric aggregates formed in a solution of lamella-former with $N_{\rm A} = N_{\rm B}/4$ mixed with a sphere-former with $N_{\rm A2} = 7N_{\rm B}$. The Flory parameter is set to the relatively high value of $\chi N_{\rm B} = 22.5$. The volume fractions of lamella-formers as a percentage of all copolymers are (a) 5%, (b) 15%, (c) 25% and (d) 35%. Sphere-formers are shown with thick lines, lamella-formers with thin lines. The hydrophobic components are plotted with full lines, the hydrophilic components with dashed lines, and the solvent with a dotted line.

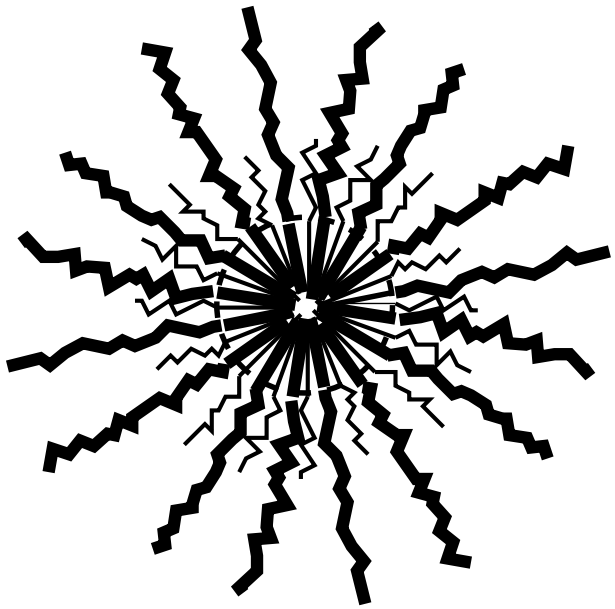

FIG. 2: Sketch of a simple mixed micelle. Sphere-formers are shown with thick lines, lamella-formers with thin lines. The hydrophobic components are plotted with straight lines, the hydrophilic components with zig-zag lines, and the boundary of the hydrophobic core is marked with a dashed circle. This structure is seen for weakly mismatched copolymers at all χ parameters considered.

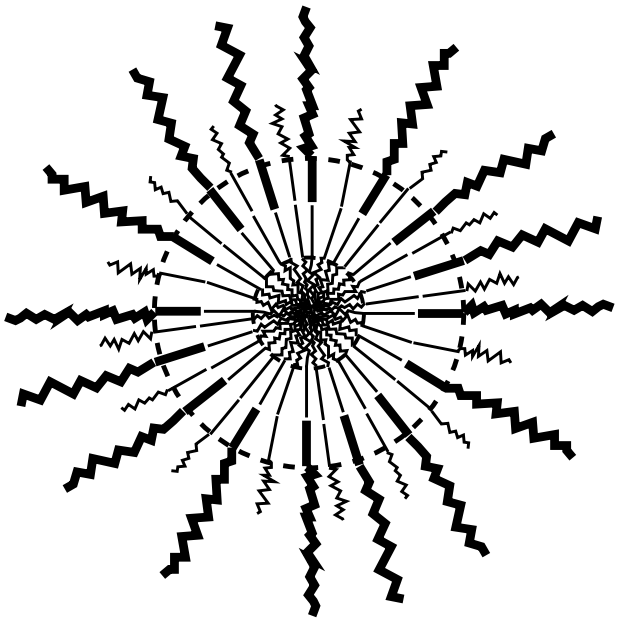

FIG. 3: Sketch of a complex ABA mixed micelle with a hydrophilic A inner core, a hydrophobic B outer core and a hydrophilic A corona. Sphere-formers are shown with thick lines, lamella-formers with thin lines. The hydrophobic components are plotted with straight lines, the hydrophilic components with zig-zag lines, and the boundaries of the two cores are marked with dashed circles. This structure is seen for larger χ parameters.

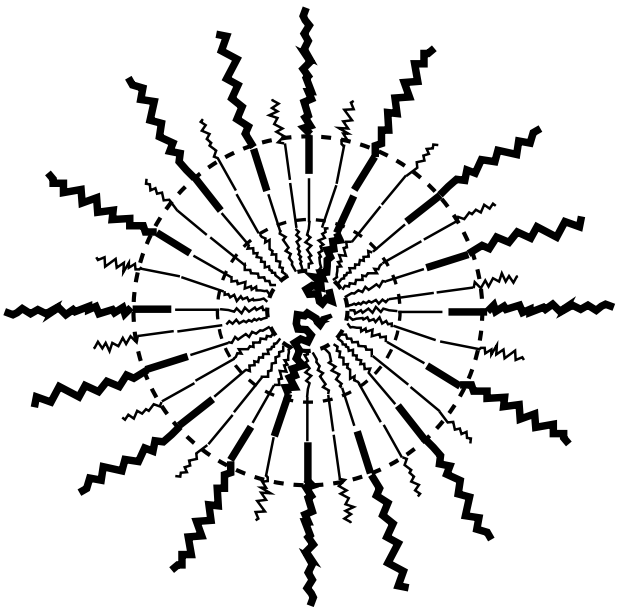

FIG. 4: Sketch of a small vesicle composed of a solvent center, a layer of hydrophilic A-blocks, a layer of hydrophobic B-blocks and a hydrophilic A corona. Sphere-formers are shown with thick lines, lamella-formers with thin lines. The hydrophobic components are plotted with straight lines, the hydrophilic components with zig-zag lines, and the boundaries of the various regions are marked with dashed circles. This structure is seen for larger χ parameters.

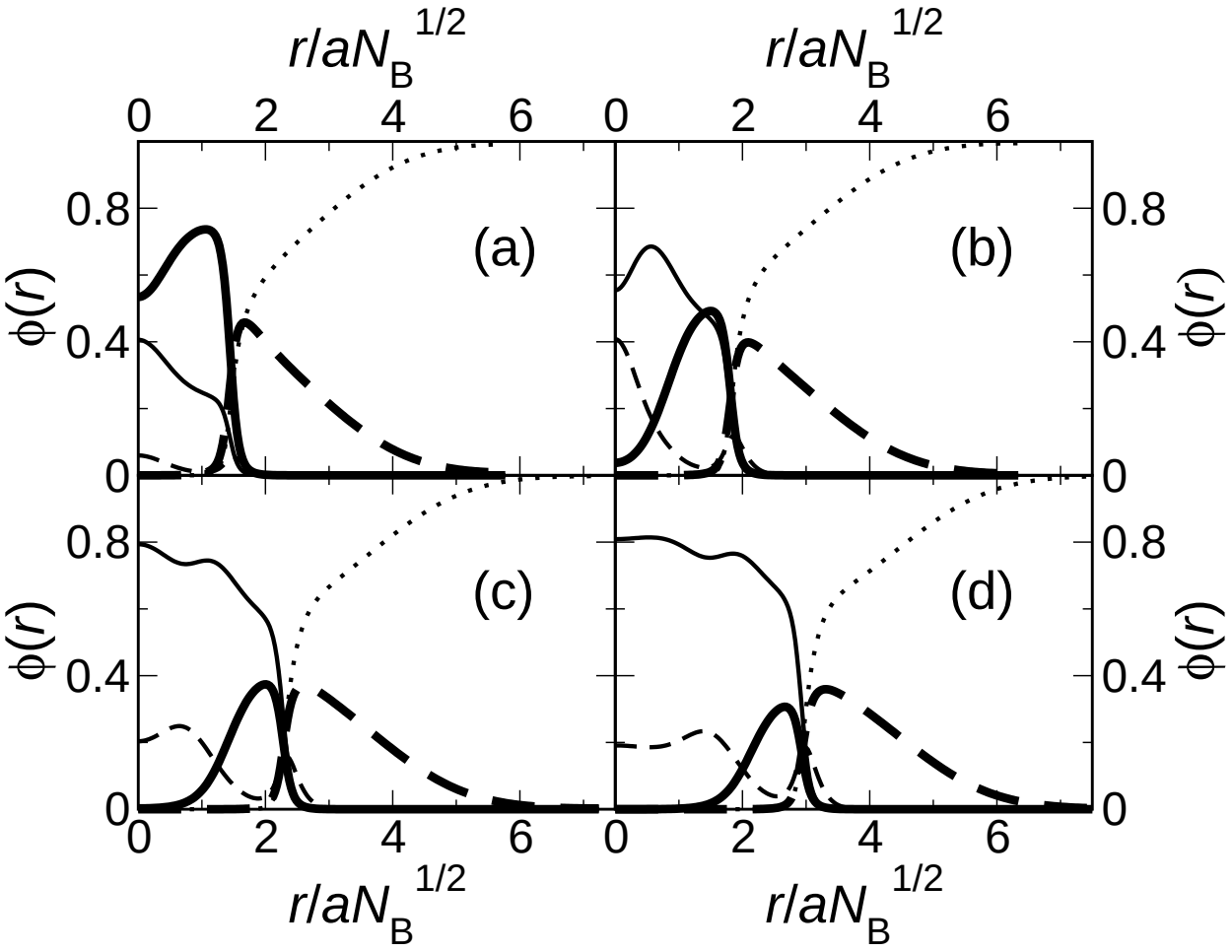

FIG. 5: Cuts through the density profiles of the spherically-symmetric aggregates formed in a solution of lamella-former with $N_{\rm A} = N_{\rm B}/4$ mixed with a sphere-former with $N_{\rm A2} = 7N_{\rm B}$. The Flory parameter is set to the relatively low value of $\chi N_{\rm B} = 15$. The volume fractions of lamella-formers as a percentage of all copolymers are (a) 5%, (b) 15%, (c) 25% and (d) 35%. Sphere-formers are shown with thick lines, lamella-formers with thin lines. The hydrophobic components are plotted with full lines, the hydrophilic components with dashed lines, and the solvent with a dotted line.

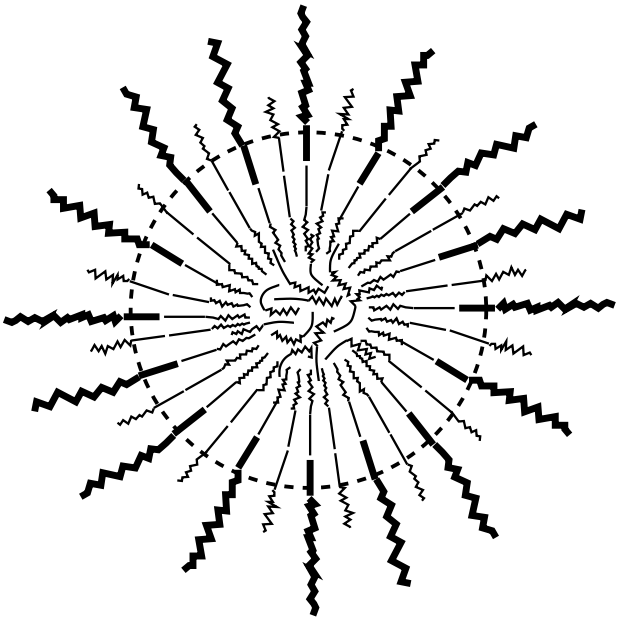

FIG. 6: Sketch of a complex mixed micelle with a weakly structured core formed of lamella-formers and the hydrophobic blocks of sphere-formers. Sphere-formers are shown with thick lines, lamella-formers with thin lines. The hydrophobic components are plotted with straight lines, the hydrophilic components with zig-zag lines, and the boundaries of the hydrophobic core is marked with a dashed circle. This aggregate is seen for lower χ parameters.

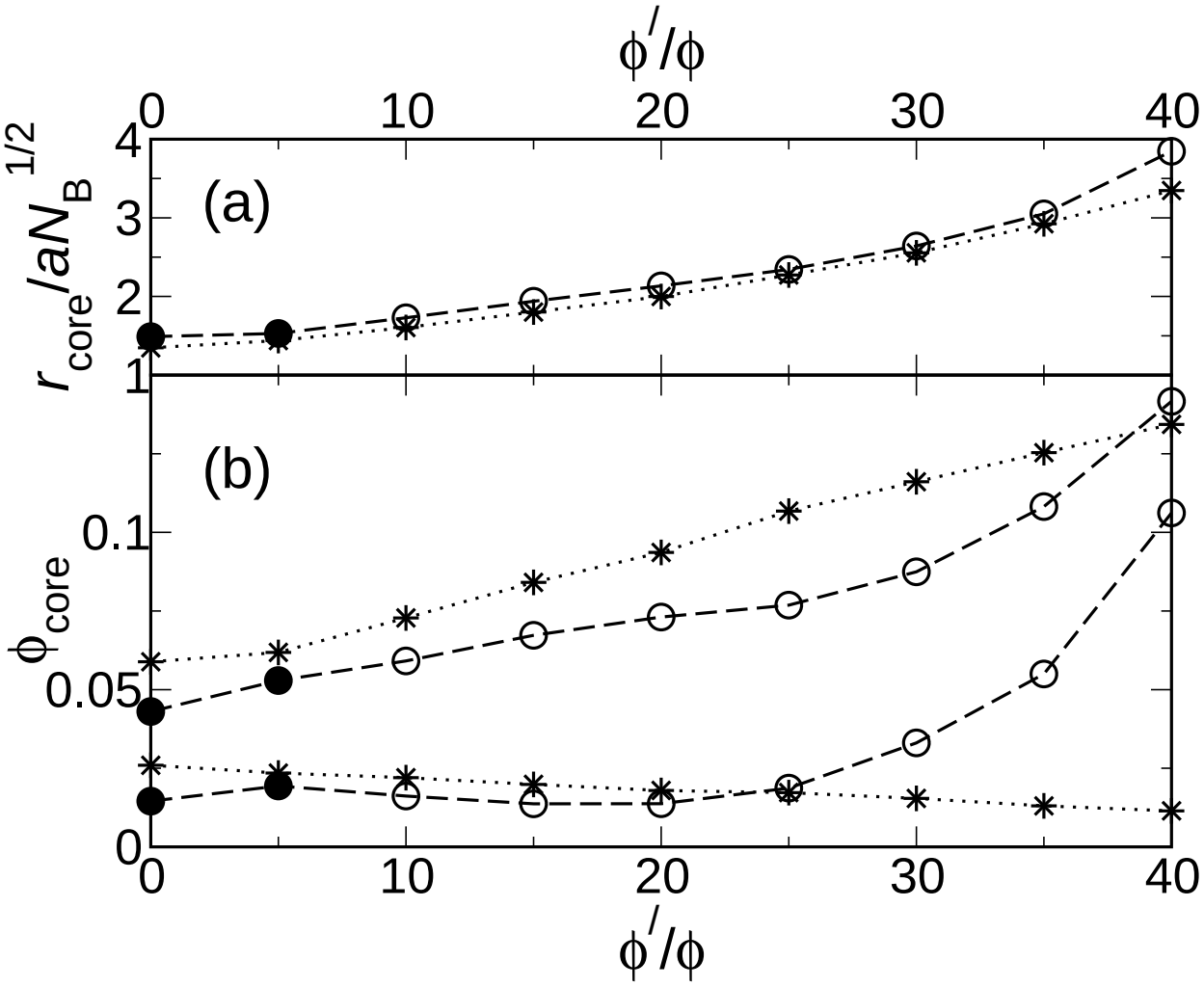

FIG. 7: Core radius and composition of the spherically-symmetric aggregates formed in a solution of lamella-former with $N_A = N_B/4$ mixed with a sphere-former with $N_{A2} = 7N_B$. (a) Core radius as a function of the ratio ϕ'/ϕ of the volume fraction of lamella-formers ϕ' to the total volume fraction of copolymers ϕ. Points corresponding to simple micelles (Figure 2) are marked by closed circles, ABA aggregates (Figure 3) or small vesicles (Figure 4) are marked with open circles, and weakly-structured aggregates (Figure 6) by asterisks. The data for the system with a Flory parameter of $\chi N_B = 15$ are connected with dotted lines; those for the system with $\chi N_B = 22.5$ by dashed lines. (b) Fraction of the core that is composed of A-blocks for each of the two systems (upper two curves), and fraction of the core that is composed of homopolymer solvent (lower two curves).

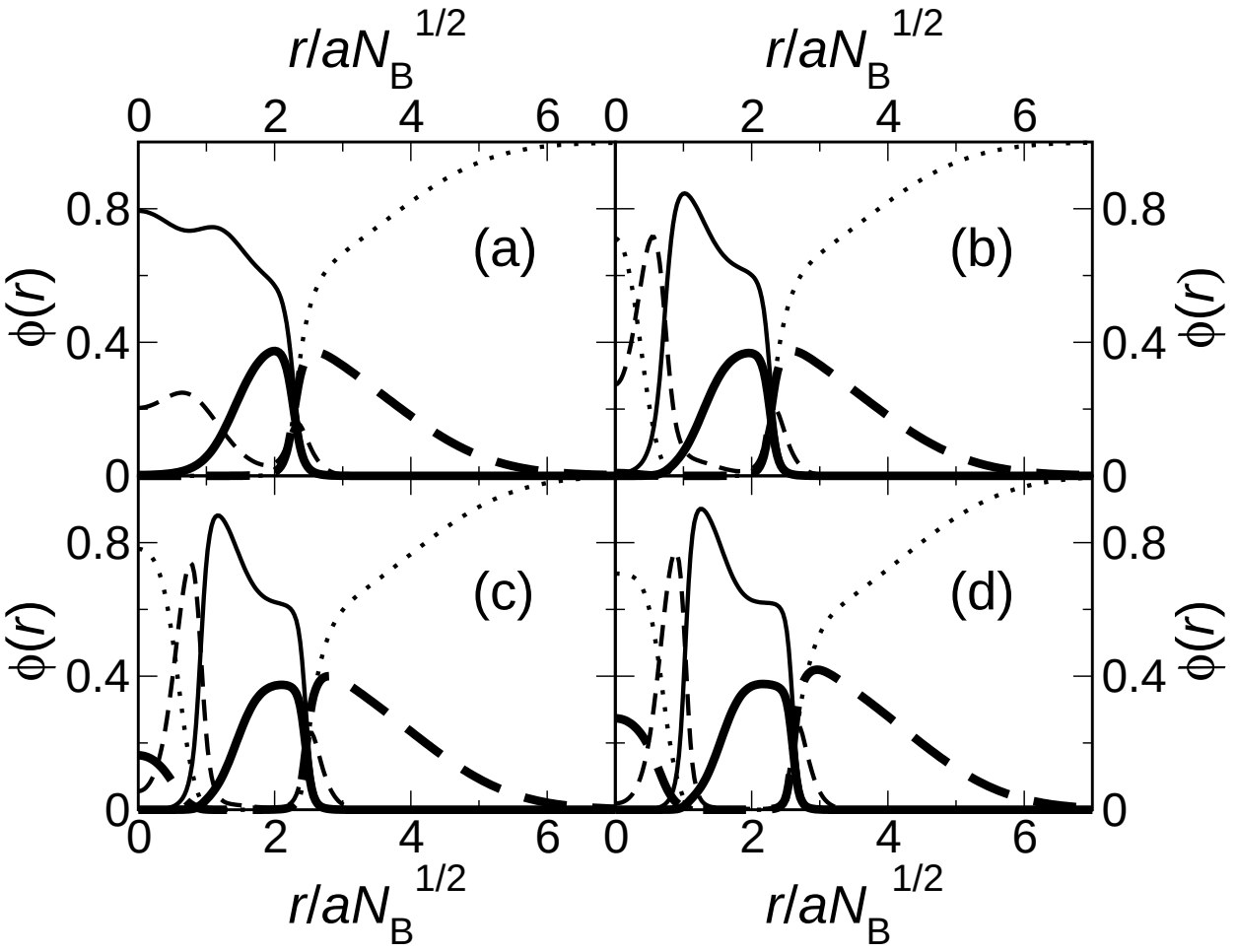

FIG. 8: Cuts through the density profiles of the spherically-symmetric aggregates formed in a solution of lamella-former with $N_{\rm A} = N_{\rm B}/4$ mixed with a sphere-former with $N_{\rm A2} = 7N_{\rm B}$. The lamella-former fraction ϕ'/ϕ is set to 25%. The Flory parameter $\chi N_{\rm B}$ is varied and takes the following values: (a) 15, (b) 20, (c) 25 and (d) 30. Sphere-formers are shown with thick lines, lamella-formers with thin lines. The hydrophobic components are plotted with full lines, the hydrophilic components with dashed lines, and the solvent with a dotted line.

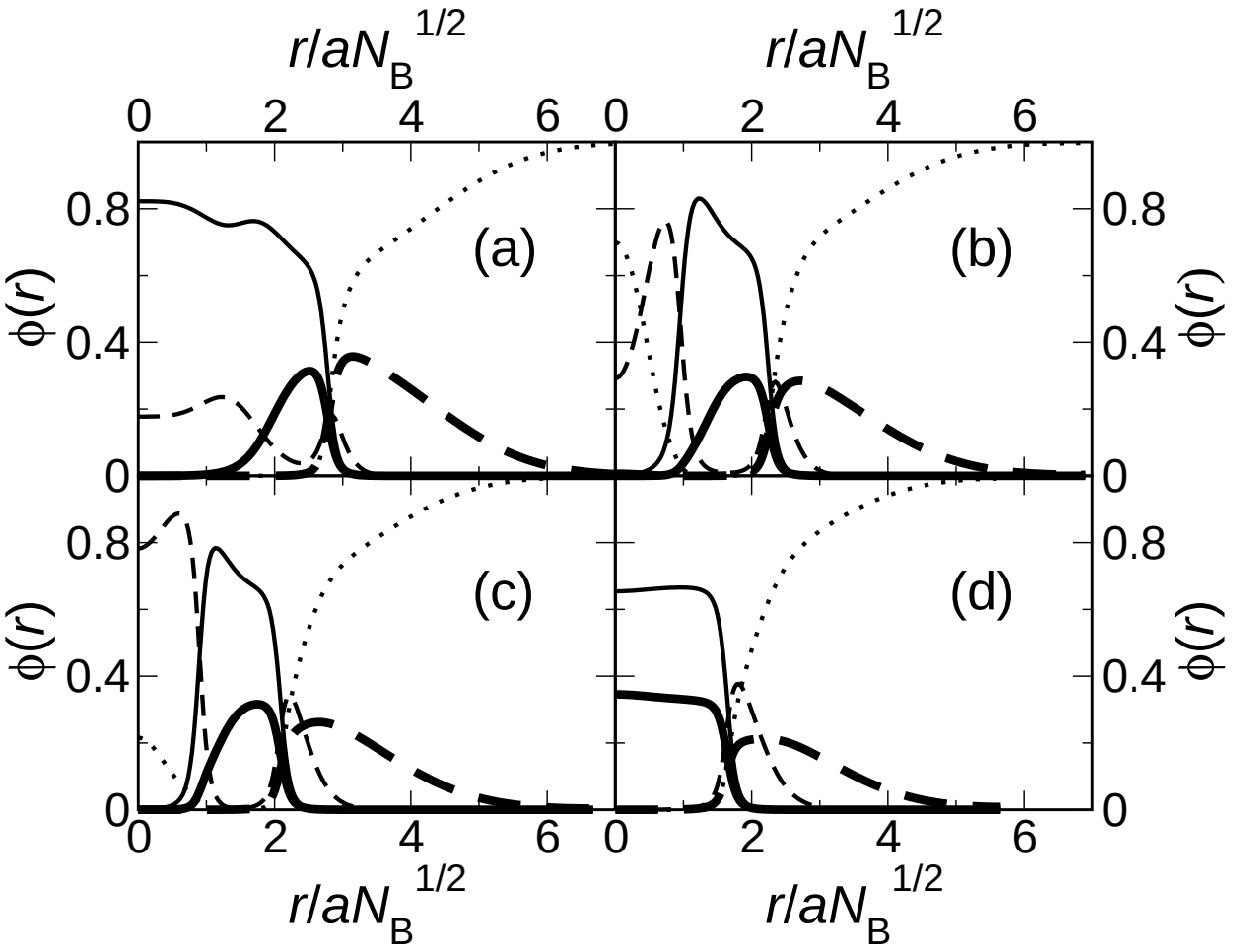

FIG. 9: Cuts through the density profiles of the spherically-symmetric aggregates formed in a solution of sphere-former with $N_{A2} = 7N_B$ and lamella-formers of varying architecture. The Flory parameter is set to the relatively low value of $\chi N_B = 15$. The lamella-former fraction ϕ'/ϕ is set to 33.3%. The hydrophilic block lengths of the lamella-forming molecules are (a), $N_A = N_B/4$ (b) $N_A = 3N_B/7$, (c) $N_A = 2N_B/3$ and (d) $N_A = N_B$. Sphere-formers are shown with thick lines, lamella-formers with thin lines. The hydrophobic components are plotted with full lines, the hydrophilic components with dashed lines, and the solvent with a dotted line.

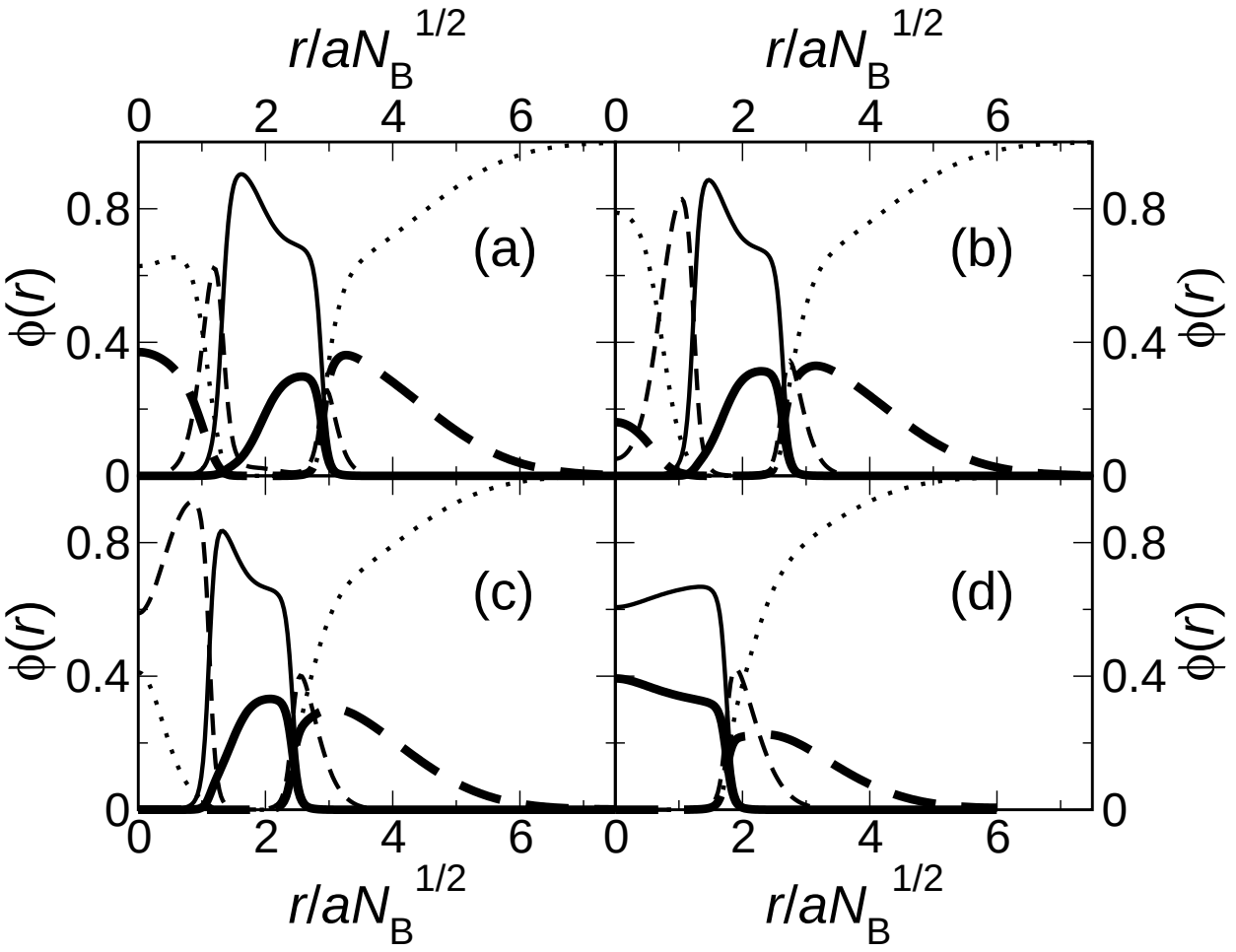

FIG. 10: Cuts through the density profiles of the spherically-symmetric aggregates formed in a solution of sphere-former with $N_{A2} = 7N_B$ and lamella-formers of varying architecture. The Flory parameter is set to the relatively high value of $\chi N_B = 22.5$. The lamella-former fraction ϕ'/ϕ is set to 33.3%. The hydrophilic block lengths of the lamella-forming molecules are (a), $N_A = N_B/4$ (b) $N_A = 3N_B/7$, (c) $N_A = 2N_B/3$ and (d) $N_A = N_B$. Sphere-formers are shown with thick lines, lamella-formers with thin lines. The hydrophobic components are plotted with full lines, the hydrophilic components with dashed lines, and the solvent with a dotted line.

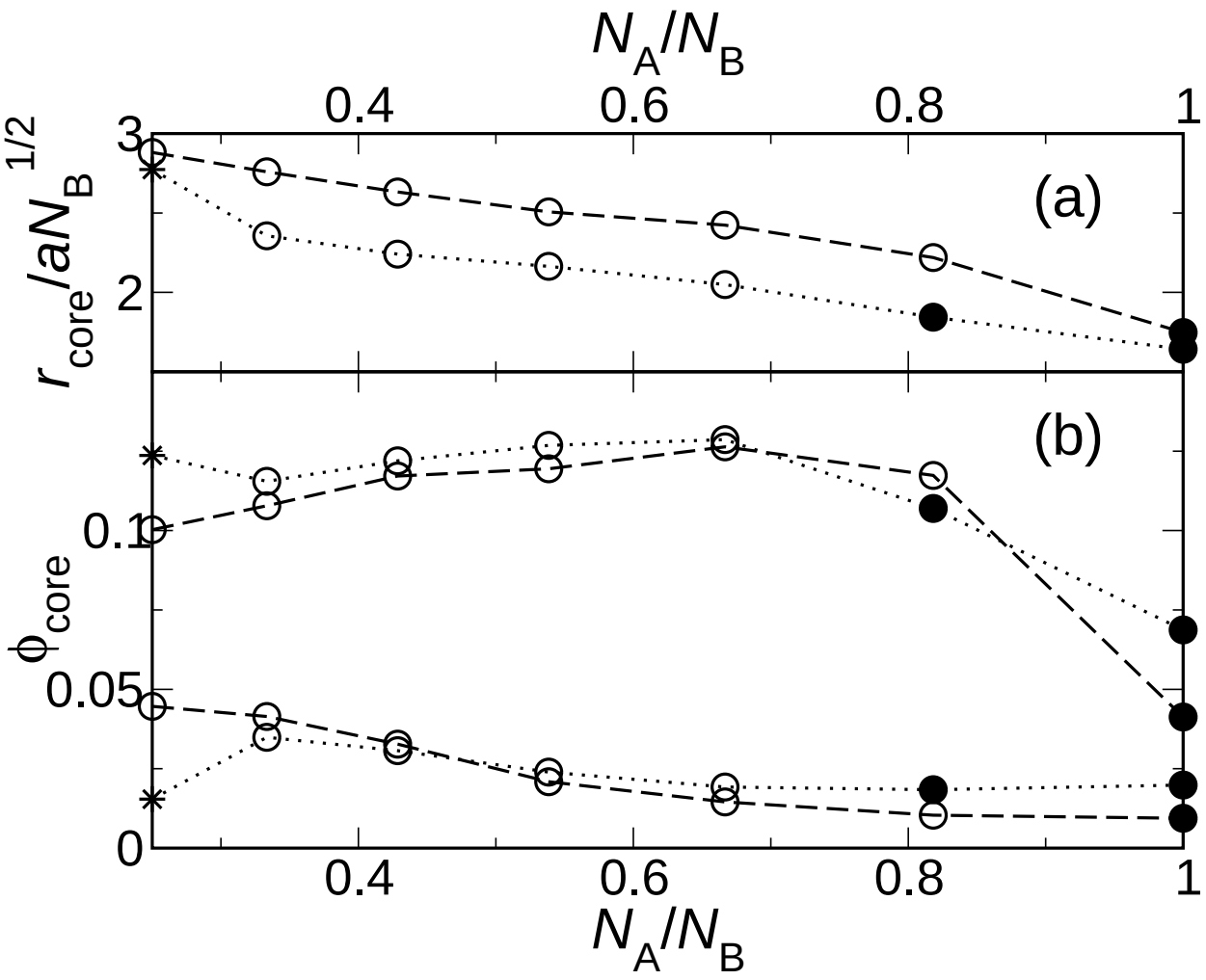

FIG. 11: Core radius and composition of the spherically-symmetric aggregates formed in a solution of sphere-former with $N_{A2} = 7N_B$ mixed with lamella-formers of various architectures. The lamella-former fraction ϕ'/ϕ is set to 33.3%. (a) Core radius as a function of the hydrophilic block length. Points corresponding to simple micelles (Figure 2) are marked by closed circles, ABA aggregates (Figure 3) or small vesicles (Figure 4) are marked with open circles, and weakly-structured aggregates (Figure 6) by asterisks. The data for the system with a Flory parameter of $\chi N_B = 15$ are connected with dotted lines; those for the system with $\chi N_B = 22.5$ by dashed lines. (b) Fraction of the core that is composed of A-blocks for each of the two systems (upper two curves), and fraction of the core that is composed of homopolymer solvent (lower two curves).

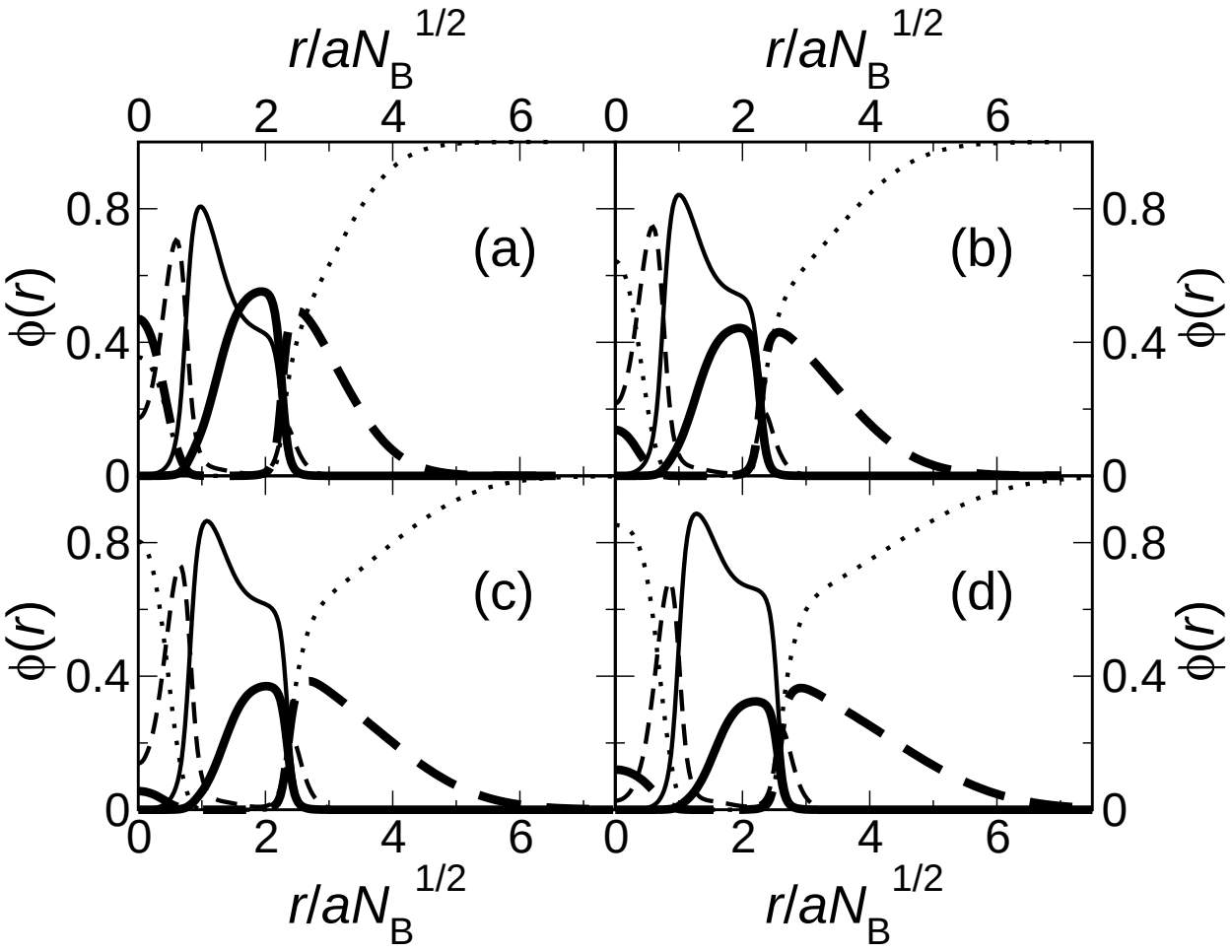

FIG. 12: Cuts through the density profiles of the spherically-symmetric aggregates formed in a solution of lamella-former with $N_{\rm A} = N_{\rm B}/4$ and sphere-formers of varying architecture. The Flory parameter is set to the relatively high value of $\chi N_{\rm A} = 22.5$. The lamella-former fraction ϕ'/ϕ is set to 25%. The hydrophilic lengths of the sphere-forming molecules are (a), $N_{\rm A2} = 3N_{\rm B}$ (b) $N_{\rm A2} = 5N_{\rm B}$, (c) $N_{\rm A2} = 7N_{\rm B}$ and (d) $N_{\rm A2} = 9N_{\rm B}$. Sphere-formers are shown with thick lines, lamella-formers with thin lines. The hydrophobic components are plotted with full lines, the hydrophilic components with dashed lines, and the solvent with a dotted line.

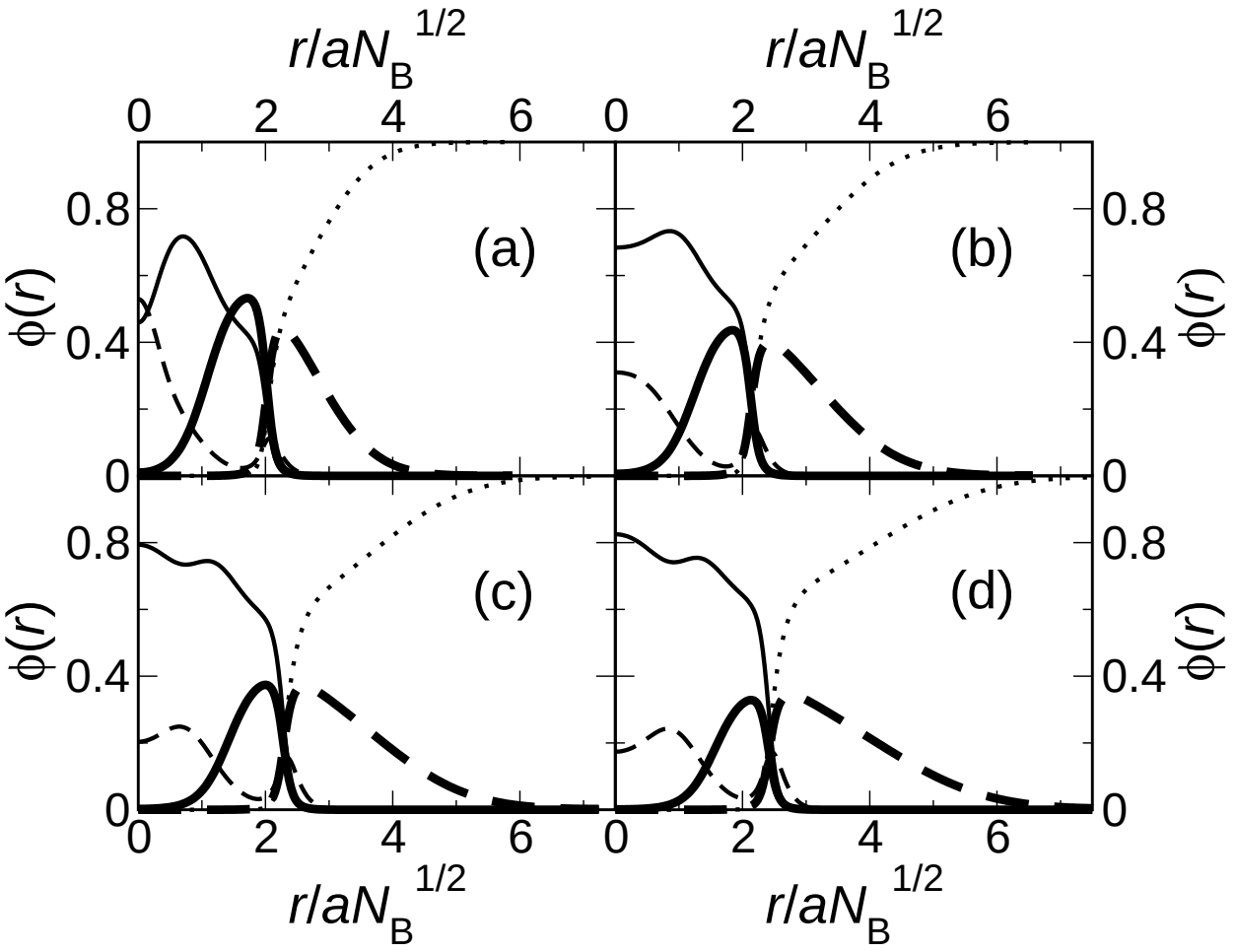

FIG. 13: Cuts through the density profiles of the spherically-symmetric aggregates formed in a solution of lamella-former with $N_{\rm A} = N_{\rm B}/4$ and sphere-formers of varying architecture. The Flory parameter is set to the relatively low value of $\chi N_{\rm B} = 15$. The lamella-former fraction ϕ'/ϕ is set to 25%. The hydrophilic lengths of the sphere-forming molecules are (a), $N_{\rm A2} = 3N_{\rm B}$ (b) $N_{\rm A2} = 5N_{\rm B}$, (c) $N_{\rm A2} = 7N_{\rm B}$ and (d) $N_{\rm A2} = 9N_{\rm B}$. Sphere-formers are shown with thick lines, lamella-formers with thin lines. The hydrophobic components are plotted with full lines, the hydrophilic components with dashed lines, and the solvent with a dotted line.

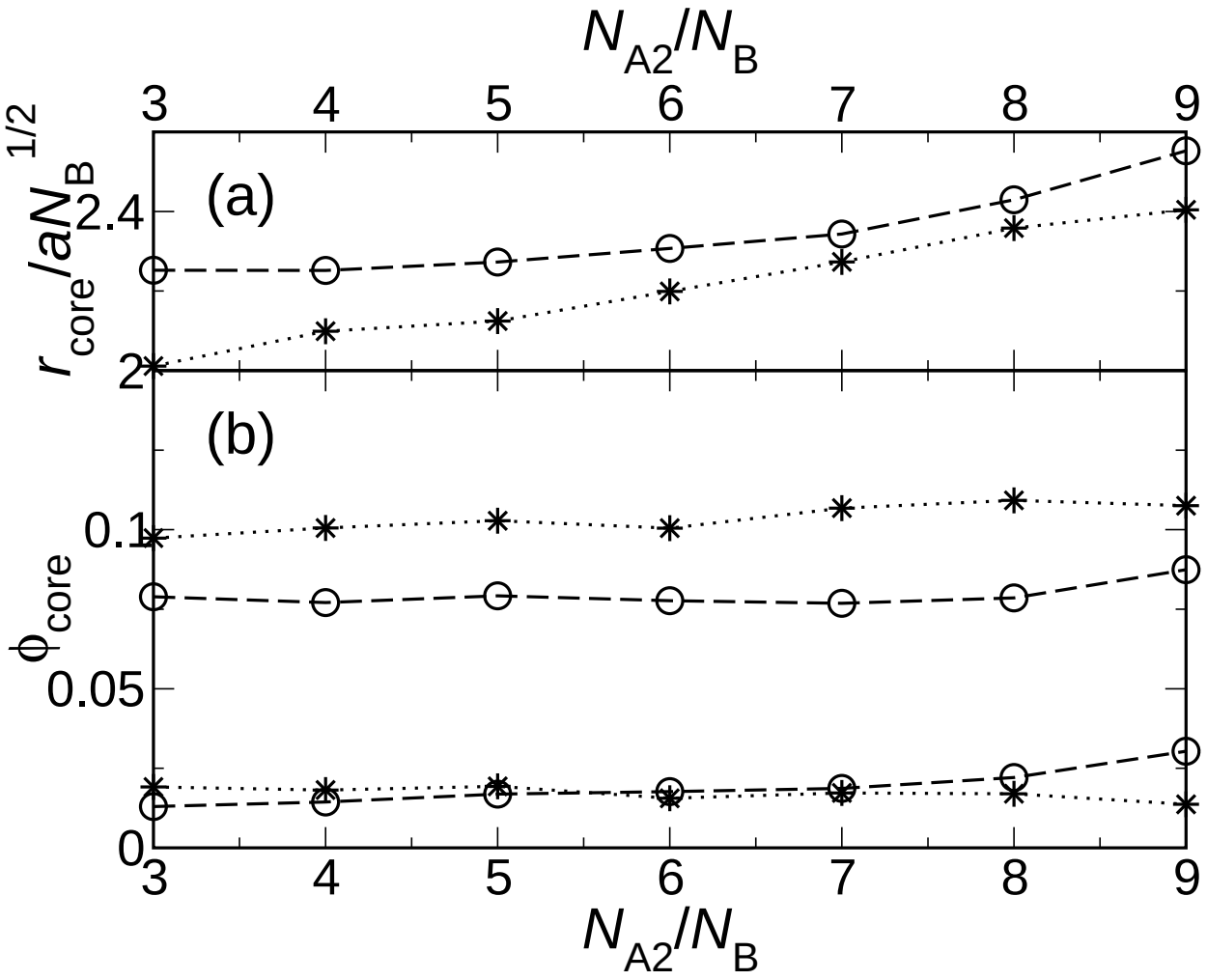

FIG. 14: Core radius and composition of the spherically-symmetric aggregates formed in a solution of lamella-former with $N_A = N_B/4$ mixed with sphere-formers of various architectures. The lamella-former fraction ϕ'/ϕ is set to 25%. (a) Core radius as a function of the hydrophilic block length. Points corresponding to simple micelles (Figure 2) are marked by closed circles, ABA aggregates (Figure 3) or small vesicles (Figure 4) are marked with open circles, and weakly-structured aggregates (Figure 6) by asterisks. The data for the system with a Flory parameter of $\chi N_B = 15$ are connected with dotted lines; those for the system with $\chi N_B = 22.5$ by dashed lines. (b) Fraction of the core that is composed of A-blocks for each of the two systems (upper two curves), and fraction of the core that is composed of homopolymer solvent (lower two curves).